Analysis of Boundary Layer Flow Second-Grade Hybrid Nanofluid Subject to Lorentz Force

Stephen Njoroge Chege[1], Maurine Wafula.[2]

[1]Department of Mathematics and Actuarial Science, Kenyatta University.

[2]School of Science and Technology, United States International University.

DOI: https://doi.org/10.51584/IJRIAS.2024.90201

Received: 16 January 2024; Accepted: 22 January 2024; Published: 26 February 2024

ABSTRACT

The suspension of nanoparticles in a fluid has been a sure way of steadily improving fluid behaviour. A further improvement in the fluid behaviour is achieved by the suspension of two dissimilar nanoparticles in a base fluid. This study analyses the boundary layer flow of second-grade hybrid nanofluid subject to Lorentz force. By considering Titanium Oxide and Molybdenum disulfide nanoparticles, due to their great lubricating and efficient heat transfer properties, the governing non-linear equations are formulated and rendered dimensionless with the help of similarity variables. The resulting boundary condition equations are transformed to initial condition equations by use of shooting technique and numerically solved by 4th-order Runge Kutta method in MATLAB bvp4c. It is noted that the fluid's velocity profile increases with the increase in volume fraction and fluctuates with increasing fluid parameters and magnetic strength. The temperature profile grows with the Prandtl number and magnetic field and decreases with the increase in volume fraction and the second-grade fluid parameter.

Nomenclature

u, v velocity in the x, y-direction respectively	P fluid density
ν kinematic viscosity	c_p coefficient of specific heat capacity
T_∞ temperature in the free stream region	α coefficient of thermal diffusivity
λ second-grade fluid parameter	T temperature
σ coefficient of electric conductivity	ß magnetic field strength
μ dynamic viscosity	

INTRODUCTION

In general, fluids have weak thermophysical characteristics. Choi and Eastman [1] proposed nanofluids as a means to improve this. This is the process of dispersing tiny particles (of 1 to 100 nm size) in a fluid. The fluid is referred to as base fluid, and these particles are known as nanoparticles. The term "nanofluid" refers to the suspension of nanoparticles in the base fluid. Investigations consistently demonstrated that nanofluids had superior qualities to fluids. Suresh et al. [2] discovered that the suspension of two different nanoparticles in a base fluid greatly enhanced fluid property. This form of fluid was dubbed a hybrid nanofluid. Research conducted over the last decade has demonstrated that hybrid nanofluids have more enhanced thermophysical features than nanofluids [3-5].

Second-grade fluids were first studied by Roux [6], who characterised them as a class of fluids developed

ISSN No. 2454-6194 | DOI: 10.51584/IJRIAS |Volume IX Issue II February 2024

from non-Newtonian fluids. This fluid's flow region was able to hold a relationship between stress and strain tensors that was up to order-two derivative. Ayub and Zaman [7] improved the momentum equation for the second-grade fluids proposed by Gorder and Vajravelu [8]. The momentum equation derivation of a second-grade fluid proposed by [7] is currently utilised in the modelling of this fluid flow. Researchers are focusing on using the second-grade fluid as a basis fluid for different nanoparticle combinations as a result of advancements in nanotechnology. Second-grade hybrid nanofluid was the subject of research by Hayat et al. [9] over a non-linearly expanding plate. According to the study's findings, a rise in the second-grade parameter causes the velocity and temperature profiles to drop. Hayat et al. [10] also reaffirmed the inverse relationship between the velocity profile and surface thickness. Furthermore, Manjunatha et al. [11] found that the fluid boundary layer's thickness reduces with a drop in fluid resistance. Rana and Latiff [12] studied the flow of second-grade fluid in a permeable medium and deduced that industrial processes can economised by increasing permeability because permeability reduces the pressure on the surface thereby consuming minimal energy in industrial processes. Huminic and Huminic [13] worked on the movement of hybrid laminar nanofluids in surfaces of elliptical design. The study noted that the maximum performance of the magnesium oxide and multi-walled carbon nanotube combination occurred at a temperature inlet of forty degrees. Gholinia et al. [14] further added that multi-walled carbon nanotubes efficiently increase the velocity of the flow compared to single-walled carbon nanotubes. Li et al. [15], in their research on modified second-grade nanofluid, showcased that with increased Rayleigh number, the temperature surges. Çiftçi, E. [16] discovered that heat transfer in hybrid nanofluids is way better in piped surfaces compared to flat surfaces. Hussien et al. [17] noted that hybrid nanofluids have higher fluid flow resistance compared to nanofluids and traditional fluids. This resistance results in a greater decrease in the fluid's pressure. Jawad et al. [18] used Homotopy Analysis to study second-grade hybrid nanofluids. The study revealed increasing the volume fraction results in a decrease in the primary velocity. Arif et al. [17] agrees with these results and further comments that the volume fraction increase also reduces the temperature profiles. Oke et al. [20] agrees with Hussien et al. [17] and demonstrates that the magnetic influence on the hybrid fluid increases the flow resistance resulting in a reduction in fluid movement rate. Juma et al. [21] concurs with the results and suggested the decrease of the magnetism to achieve faster heat transfer. Juma et al. [22] noted that in a rotating plate, the drag reduces with increasing surface rotation. Nadeem et al. [23] also notes that volume fraction has a direct proportionality with the heat transfer rate of the second-grade hybrid nanofluid. Siddique et al. [24] displays that hybrid nanofluid heat transmission is quicker compared to the second-grade fluid which can be attributed to surface thickness. This implies that when the surface thickness is large, the hybrid nanofluid conducts heat faster. Reddy et al. [25] concurs with results posted by Çiftçi E. [6] that better heat transmission in piped surfaces compared to flat surfaces. Further, Reddy et al. [25] generalises that this is true for all curved surfaces, not just pipe surfaces.

From the literature review above, it is notably obvious that hybrid nanofluids have been of major interest to researchers. So far, multiple studies have been done on first-grade hybrid nanofluid flow. Little research has been done on second-grade hybrid nanofluids but, no researcher has considered the influence of Lorentz force on a second-grade hybrid nanofluid. To bridge this gap, this study analyses the boundary layer flow of second-grade hybrid nanofluid subject to Lorentz force. The flow is on a surface of uniform thickness. The surface is linearly stretching horizontally and the fluid flow is experiencing perpendicular magnetic influence. The nanoparticles used are Titanium Oxide and Molybdenum disulfide.

METHODOLOGY

The flow of a hybrid nanofluid is investigated over an infinitely long horizontal surface. A second-grade fluid is used as the base fluid while carrying Titanium Oxide and Molybdenum disulphide nanoparticles are suspended in the base fluid. The colloidal suspension is homogeneously mixed in a single phase so that the law of continuum is applicable. The flow is subjected to a controlled magnetism applied perpendicular to the flow. Figure (1) depicts the physical configuration of the boundary layer section of the flow. In this

ISSN No. 2454-6194 | DOI: 10.51584/IJRIAS |Volume IX Issue II February 2024

section, the assumptions and equations governing the flow are highlighted.

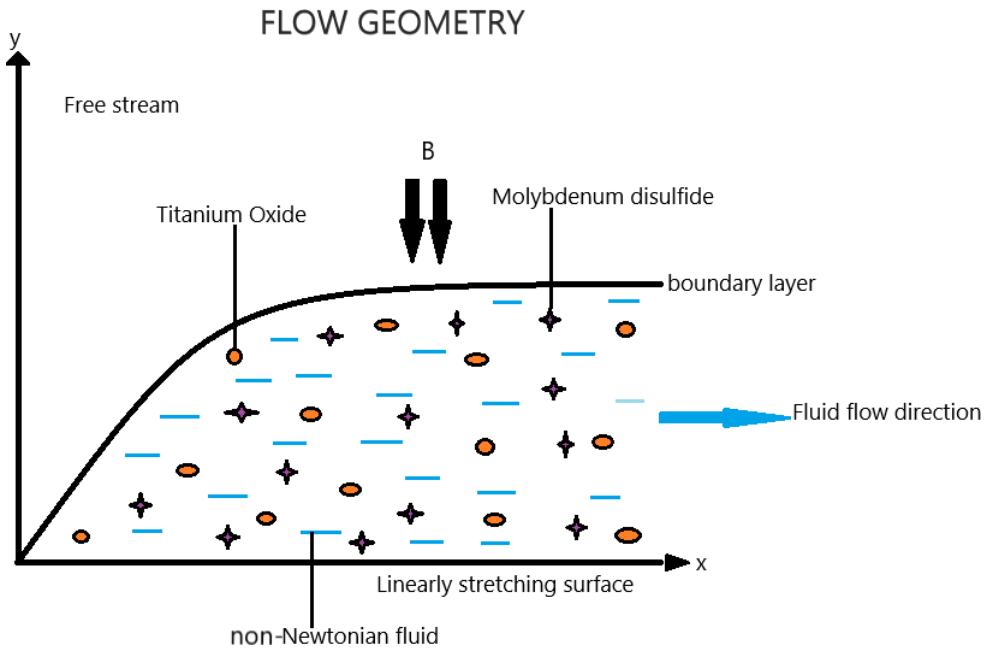

Figure 1: Flow description

The equations governing the flow are modelled according to Navier-Stokes equations. According to Koriko et al. [26], the general continuity equation is:

$$\frac{\partial}{\partial t}\rho(t,\boldsymbol{x}) + \nabla\cdot\left(\rho\left(u_1(t,\boldsymbol{x})\hat{\imath} + u_2(t,\boldsymbol{x})\hat{\jmath} + u_3(t,\boldsymbol{x})\hat{k}\right)\right) = 0. \quad (1)$$

where $\boldsymbol{x} = (x_1, x_2, x_3)$, $V = (u_1, u_2, u_3)$ For steady incompressible flow, time derivative vanishes and $\rho\ (t, \boldsymbol{x}) = \rho$ is constant and also, for a 2D flow, $\boldsymbol{x} = (x_1, x_2)$ and $u_3 = 0$ Hence, equation (1) becomes

$$\nabla\cdot(u_1(x_1,x_2)\hat{\imath} + u_2(x_1,x_2)\hat{\jmath}) = 0$$

and the continuity equation is

$$\frac{\partial u_1}{\partial x_1} + \frac{\partial u_2}{\partial x_2} = 0. \quad (2)$$

Following Oke [27], the equation for the conservation of momentum is:

$$\rho\left(\frac{\partial \boldsymbol{V}}{\partial t} + (\boldsymbol{V}\cdot\nabla)\boldsymbol{V}\right) = \nabla\cdot\boldsymbol{\sigma} + \rho B,$$

where $\boldsymbol{\sigma}$ is the stress tensor and **B** represents the body forces. Ignoring the time derivative then,

$$\rho(\boldsymbol{V}\cdot\nabla)\boldsymbol{V} = \nabla\cdot\boldsymbol{\sigma} + \rho B.$$

Ayub and Zaman [7] gave the stress tensor for the second-grade fluid as

$$\boldsymbol{\sigma} = -p\boldsymbol{I} + \mu\boldsymbol{A}_1 + \alpha_1\boldsymbol{A}_2 + \alpha_2\boldsymbol{A}_1^2 \quad (3)$$

where $\boldsymbol{I}$, p and $\mu \geq 0$ are the identity tensor, pressure and dynamic viscosity; α_1 and α_2 are material constants

ISSN No. 2454-6194 | DOI: 10.51584/IJRIAS |Volume IX Issue II February 2024

such that $\alpha_1 \geq 0,\ \alpha_1 + \alpha_2 = 0$; and $\boldsymbol{A}_1, \boldsymbol{A}_2$ are Rivillin Ericksen tensors defined as

$$\boldsymbol{A}_1 = \nabla \boldsymbol{V} + (\nabla \boldsymbol{V})^T, \quad \boldsymbol{A}_2 = \frac{\partial \boldsymbol{A}_1}{\partial t} + (\boldsymbol{V} \cdot \nabla)\boldsymbol{A}_1 + \boldsymbol{A}_1(\nabla \boldsymbol{V}) + (\nabla \boldsymbol{V})^T \boldsymbol{A}_1.$$

However, since the flow is steady, the time derivatives are zeros and we have

$$\boldsymbol{A}_2 = (\boldsymbol{V} \cdot \nabla)\boldsymbol{A}_1 + \boldsymbol{A}_1(\nabla \boldsymbol{V}) + (\nabla \boldsymbol{V})^T \boldsymbol{A}_1 = (\boldsymbol{V} \cdot \nabla)\boldsymbol{A}_1 + \boldsymbol{A}_1(\nabla \boldsymbol{V}) + (\boldsymbol{A}_1^T \nabla \boldsymbol{V})^T. \tag{4}$$

According to Beard (1964) and Andersson, H. I. (1992), the momentum and energy equations are

$$u\frac{\partial u}{\partial x} + v\frac{\partial u}{\partial y} = \vartheta_{bf}\frac{\partial^2 u}{\partial y^2} + \lambda\left(\frac{\partial}{\partial x}\left(u\frac{\partial^2 u}{\partial y^2}\right) + \frac{\partial u}{\partial y}\frac{\partial^2 u}{\partial x \partial y} + v\frac{\partial^3 u}{\partial y^3}\right) - \frac{\sigma_{hnf}}{\rho_{hnf}}B^2 u, \tag{5}$$

$$u\frac{\partial T}{\partial x} + v\frac{\partial T}{\partial y} = \frac{\kappa_{hnf}}{(\rho C_p)_{hnf}}\frac{\partial^2 T}{\partial y^2}. \tag{6}$$

The no-slip condition gives the boundary conditions

$$u = cx, \qquad v = 0, \qquad T = T_w \tag{7}$$

$$u \to 0, \frac{\partial u}{\partial y} = 0, T \to T_\infty \tag{8}$$

The effective properties of electrical conductivity and density of the nanofluid are given as

$$\sigma_{hnf} = \left(1 - \phi + \frac{1}{\sigma_{bf}}\sum_{i=1}^{2}\phi_i\sigma_i\right)\sigma_{bf}, \quad \rho_{hnf} = \left(1 - \phi + \frac{1}{\rho_{bf}}\sum_{i=1}^{2}\phi_i\rho_i\right)\rho_{bf}.$$

$$\frac{\kappa_{hnf}}{\kappa_{bf}} = \frac{(1+2\phi)(\sum_{i=1}^{2}\phi_i\kappa_i) + 2(1-\phi)\phi\kappa_{bf}}{(1-\phi)(\sum_{i=1}^{2}\phi_i\kappa_i) + (2+\phi)\phi\kappa_{bf}}$$

$$(\rho C_p)_{hnf} = \left(1 - \phi + \frac{1}{(\rho C_p)_{bf}}\sum_{i=1}^{2}\phi_i(\rho C_p)_i\right)(\rho C_p)_{bf}$$

Transformation using similarity variables

Consider the stream function and the similarity variable

$$\psi = \sqrt{c\vartheta_{bf}}xf(\eta), \ \eta = y\sqrt{\frac{c}{\vartheta_{bf}}}, \ T = T_w + (T_\infty - T_w)\Theta,$$

with the condition that

$$\frac{\partial u}{\partial x} = -\frac{\partial v}{\partial y}$$

Then,

$$u = cxf'^{(\eta)}, \quad v = -\sqrt{c\vartheta_{bf}}f(\eta), \quad T = T_w + (T_\infty - T_w)\Theta.$$

Hence, the dimensionless equations are

ISSN No. 2454-6194 | DOI: 10.51584/IJRIAS |Volume IX Issue II February 2024

$$ff'' - (f')^2 + f''' + \lambda_1(2f'f''' + (f'')^2) + \frac{A_1 M}{A_2} f' - \lambda_1 f f^{iv} = 0. \quad (9)$$

$$B_1\Theta'' + B_2 Prf\Theta' = 0. \quad (10)$$

with the conditions

$$f'^{(0)} = 1, \quad f(0) = 0, \quad \Theta(0) = 0, \quad (11)$$

$$f'^{(\infty)} = 0, \quad f''^{(\infty)} = 0, \quad \Theta(\infty) = 1 \quad (12)$$

and

$$A_1 = \left(1 - \phi + \frac{1}{\sigma_{bf}} \sum_{i=1}^{2} \phi_i \sigma_i\right), \quad A_2 = \left(1 - \phi + \frac{1}{\rho_{bf}} \sum_{i=1}^{2} \phi_i \rho_i\right),$$

$$B_1 = \frac{(1+2\phi)(\sum_{i=1}^{2} \phi_i \kappa_i) + 2(1-\phi)\phi\kappa_{bf}}{(1-\phi)(\sum_{i=1}^{2} \phi_i \kappa_i) + (2+\phi)\phi\kappa_{bf}},$$

$$B_2 = \left(1 - \phi + \frac{1}{(\rho C_p)_{bf}} \sum_{i=1}^{2} \phi_i (\rho C_p)_i\right),$$

$$\lambda_1 = \frac{\lambda_c}{\vartheta_{bf}}, \ \frac{\sigma_{hnf} B^2}{c\rho_{hnf}} = \frac{A_1 \sigma_{bf} B^2}{c A_2 \rho_{bf}} = \frac{A_1 M}{A_2}, \ M = \frac{\sigma_{bf} B^2}{c\rho_{bf}}.$$

Numerical Solution

Setting

$$g_1 = f, \ g_2 = f', \ g_3 = f'', \ g_4 = f''', \ g_5 = \Theta, \ g_6 = \Theta',$$

and the equations become

$$g_4' = \frac{g_1 g_3 - (g_2)^2 + g_4 + \lambda_1(2g_2 g_4 + g_3^2) + \frac{A_1 M}{A_2} g_2}{\lambda_1 g_1} \quad (13)$$

$$g_5' = g_6, \ g_6{}' = \frac{B_2}{B_1} Pr g_1 g_6.$$

The boundary conditions (11) and (12) are written as

$$g_1(0) = 0, g_2(0) = 1, g_5(0) = 0, \quad (14)$$

$$g_2(\infty) = 0, g_3(\infty) = 0, g_5(\infty) = 1. \quad (15)$$

Considering the equations as a system of autonomous equations

$$G' = F(G), \quad \text{where } G = (g_1, g_2, \cdots, g_6)^T$$

with the condition

$$G(0) = G_0.$$

ISSN No. 2454-6194 | DOI: 10.51584/IJRIAS |Volume IX Issue II February 2024

The equations require six initial conditions to be solved completely but only three initial conditions (i.e., $g_1(0) = 0,\ g_2(0) = 1,\ g_5(0) = 0$) are available. A complete initial condition will be

$$G_0 = (0,1, s_1, s_2, 0, s_3)^T$$

where s_1, s_2, s_3 are to be obtained by the Shooting technique so that the boundary conditions (15) (i.e., $g_2(\infty) = 0,\ g_3(\infty) = 0,\ g_5(\infty) = 1$) are satisfied [28].

ANALYSIS AND DISCUSSION OF RESULTS

The nanoparticles' thermophysical parameters are listed in Table 1. Figures (2) – (4) show the response of velocity profiles to the variations in the volume fraction, magnetic field, and second-grade fluid characteristics while temperature profiles are shown in Figures (5) – (7) in relation to the volume fraction, magnetic field, Prandtl number, and second-grade fluid parameter.

Table 1: Nanoparticles and second-grade fluid Thermophysical properties

	TiO_2	MoS_2	Blood
$\sigma(sm^{-1})$	5.5X10^{-6}	2.09X10^{4}	1090
$\rho(kgm^{-3})$	4250	5060	1050
$\kappa(Wm^{-1}K^{-1})$	8.96	904.4	0.52
$c_p(Jkg^{-1}K^{-1})$	686.2	397.21	3617
source	Hussain et al. [29]	Vinayagam and Golla [30]	Khan et al. [31]

Figure 2 shows displays the behaviour of the velocity profiles when the volume fraction increases. The momentum boundary layer thinning brought about by increasing volume fraction causes an increase in the velocity and hence, figure 2 shows that the velocity profiles increase with increasing volume fraction. Figure 3 shows a sinusoidal response of the velocity profile to the magnetic field strength. The velocity increase is caused by the reduction in the rate at which the fluid nanoparticles collide as the magnetic field strength is applied to the flow. When the collision rate goes down, the resistance offered to the flow also declines leading to higher fluid velocity. The second-grade fluid parameter increases the velocity as shown in Figure 4 due to the instability within the flow as this parameter increases.

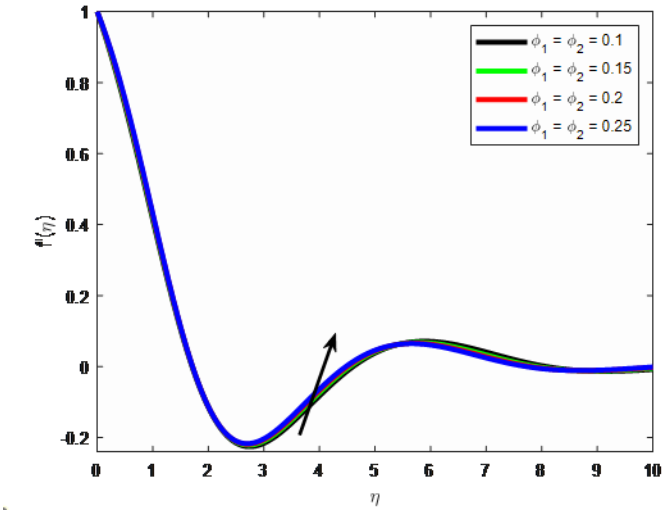

Figure 2: Velocity profile against volume fraction

ISSN No. 2454-6194 | DOI: 10.51584/IJRIAS |Volume IX Issue II February 2024

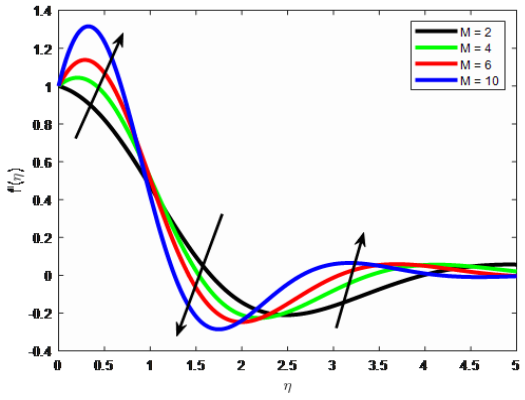

Figure 3: Velocity profile against magnetic field strength

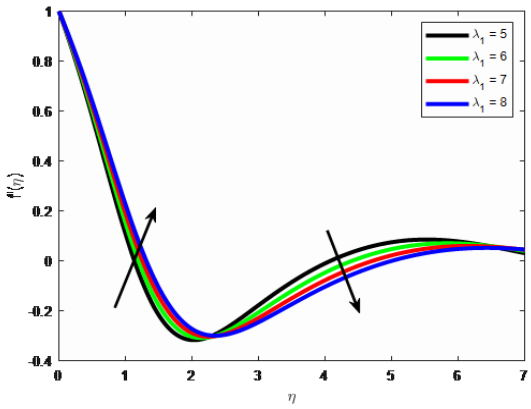

Figure 4: Velocity profile against second-grade parameter

Figure 5 shows that the temperature profile increases with Prandtl number due to increasing fluid's viscosity. Temperature declines with the growing volume fraction (see Figure 6). A slight increment in the volume fraction decreases the fluid heat conduction, and consequently lead to a reduction in temperature. Figure 7 shows a rise in the fluid temperature with magnetic parameter. Magnetic field strength increases the thermal boundary layer while reducing the momentum boundary layer. Internal energy of the flow is enhanced and there is a creation of the Lorentz force which is transferred through the fluid as thermal energy and leading to increasing flow temperature. Figure 8 shows that the temperature profile decreases with increasing second-grade fluid parameter.

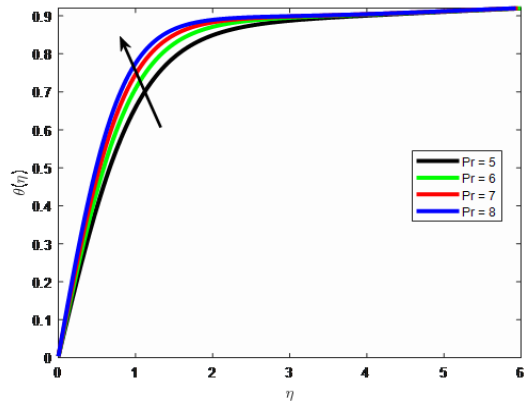

Figure 5: Temperature profile against Prandtl number

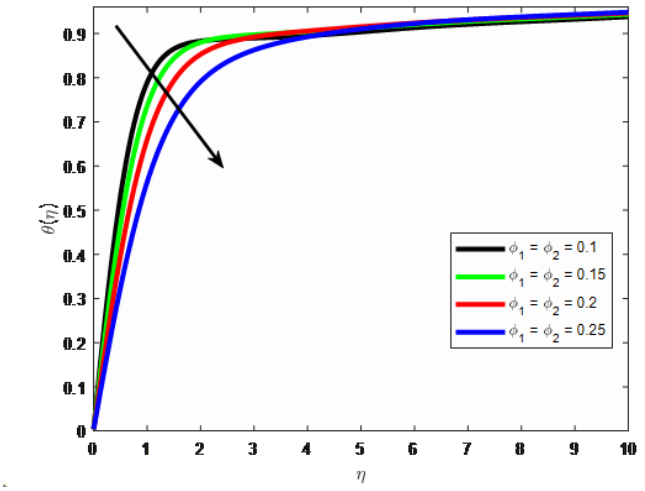

Figure 6: Temperature profile against volume fraction

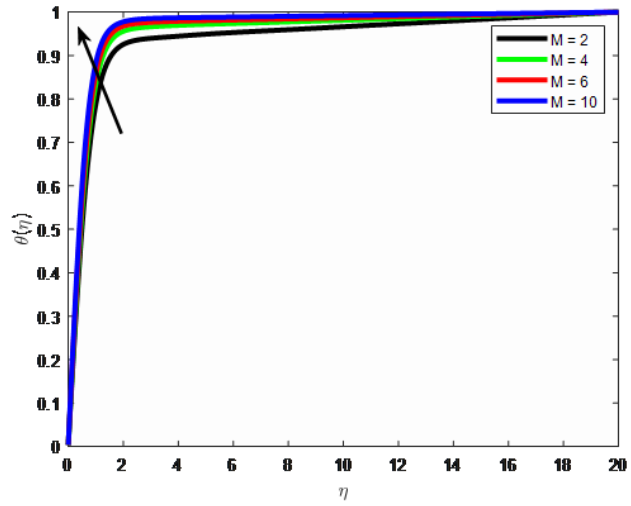

Figure 7: Temperature profile against magnetic field strength

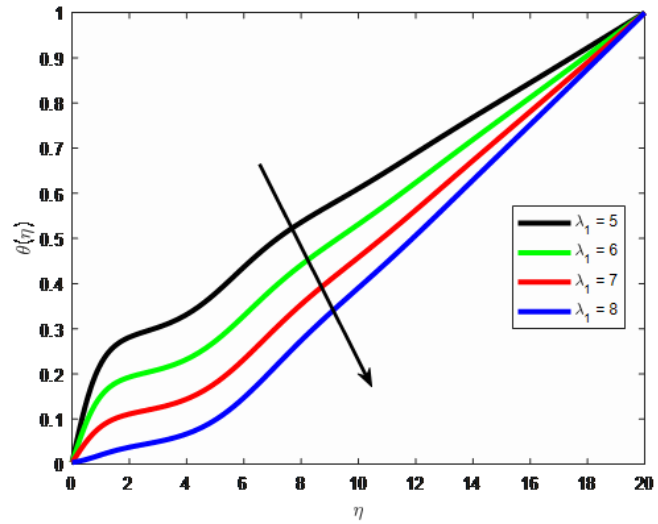

Figure 8: Temperature profile against second-grade fluid parameter

CONCLUSION

Boundary layer flow of second-grade hybrid nanofluid subject to Lorentz force is investigated in this study over a linearly stretching surface. The governing partial differential equations are developed and later transformed using the similarity variables. From the results, the following were observed;

1. velocity increases with volume fraction.
2. Temperature increases with Prandtl number and magnetic field but reduces with volume fraction and the second-grade fluid parameter.

Hence, volume fraction should be increased to increase the second-grade fluid velocity in industries. Also, high magnetic field is required to achieve higher temperature.

REFERENCES

1. Choi, U. S. & Eastman, J. (1995). Enhancing thermal conductivity of fluids with nanoparticles. *ASME International Mechanical Congress and Exposition*, 12–17.
2. Suresh S., Venkitaraj K. P., Selvakumar P. & Chandrasekar M. (2011). Synthesis of Al_2O_3-Cu/water hybrid nanofluids using two step method and its thermophysical properties. *Colloids and Surfaces A: Physiochemical and Engineering Aspects, 388*(1), 41–48.
3. Oke, A. S. (2022). Combined effects of Coriolis force and nanoparticle properties on the dynamics of gold–water nanofluid across nonuniform surface. *ZAMM-Journal of Applied Mathematics and Mechanics/Zeitschrift für Angewandte Mathematik und Mechanik*, *102*(9), e202100113.
4. Oke, A. S., Mutuku, W. N., Kimathi, M., & Animasaun, I. L. (2020). Coriolis effects on MHD newtonian flow over a rotating non-uniform surface. *Proceedings of the Institution of Mechanical Engineers, Part C: Journal of Mechanical Engineering Science, 235*(19), 3875–3887.
5. Oke, A. S., Eyinla, T., & Juma, B. A. (2023). Effect of Coriolis Force on Modified Eyring Powell Fluid flow. *Journal of Engineering Research and Reports, 24*(4), 26-34.
6. Roux, C. (1997). Second-grade fluids with slip boundary conditions. *Faculty of Science, University of Pretoria.*
7. Ayub, M. & Zaman, H. (2010). Complete derivation of the momentum equation for the second-grade fluid. *Journal of Mathematics and Computer Science, 1*(1), 33-39.
8. Gorder, R. V. & Vajravelu, K. (1999). Series solution of hydromagnetic flow and heat transfer with hall effect in a second-grade fluid over a stretching sheet. *Central European Journal of Physics*.
9. Hayat, T., Aziz, A., Muhammad, T., & Ahmad, B. (2016). On magnetohydrodynamic flow of second-grade nanofluid over a nonlinear stretching sheet. *Journal of Magnetism and Magnetic Materials, 408* , 99-106.
10. Hayat, T., Ullah, I., Alsaedi, A., & Farooq, M. (2017). MHD flow of powell-eyring nanofluid over a non-linear stretching sheet with variable thickness. *Results in Physics, 7*, 189–196.
11. Manjunatha, S., Kuttan, B. A., Jayanthi, S., Chamkha, A., & Gireesha, B. (2019). Heat transfer enhancement in the boundary layer flow of hybrid nanofluids due to variable viscosity and natural convection. *Heliyon, 5*(e01469).
12. Rana, M. & Latif, A. (2019). Three-dimensional free convective flow of a second-grade fluid through a porous medium with periodic permeability and heat transfer. *Boundary Value Problems, a Springer open journal.*
13. Huminic, G. & Huminic, A. (2019). The influence of hybrid nanofluids on the performances of elliptical tube: Recent research and numerical study. *International Journal of Heat and Mass Transfer, 129*, 132-143.
14. Gholinia, M., Hosseinzadeh, K., & Ganji, D. (2020). Investigation of different base fluids suspend by CNTs hybrid nanoparticle over a vertical circular cylinder with sinusoidal radius. *Case Studies in Thermal Engineering, 21*

(100666.).
15. Li, Y., Waqas, H., Imran, M., Farooq, U., Mallawi, F., & Tlili, I. (2020). A numerical exploration of modified second-grade nanofluid with motile microorganisms, thermal radiation, and wu's slip. *Symmetry, 12*(3), 393.
16. Çiftçi, E. (2021). Distilled water-based AlN/ ZnO binary hybrid nanofluid utilization in a heat pipe and investigation of its effects on performance. *International Journal of Thermophysics, 42*(3).
17. Hussien, A., Abdullah, M., Yusop, N., Al-Kouz, W., Mahmoudi, E., & Mehrali, M. (2021). Heat transfer and entropy generation abilities of mwcnts/gnps hybrid nanofluids in microtubes. *Entropy, 5* (21), 480.
18. Jawad, M., Saeed, A., Tassaddiq, A., Khan, A., Gul, T., Kumam, P., & Shah, Z. (2021). Insight into the dynamics of second-grade hybrid radiative nanofluid flow within the boundary layer subject to lorentz force. *Scientific Reports, 11*(1).
19. Arif, M., Saeed, A., Suttiarporn, P., Khan, W., Kumam, P., & Watthayu, W. (2022). Analysis of second-grade hybrid nanofluid flow over a stretching flat plate in the presence of activation energy. *Scientific reports, 12*(21565).
20. Oke, A., Prasannakumara, B., Mutuku, W., Gowda, R. P., Juma, B., Kumar, R. N., & Bada, O. (2022). Exploration of the effects of coriolis force and thermal radiation on water-based hybrid nanofluid flow over an exponentially stretching plate. *Scientific Reports.*
21. Juma B. A., Oke A. S., Ariwayo A. G., & Ouru O. J. (2022). Theoretical analysis of mhd williamson flow across a rotating inclined surface. *Applied Mathematics and Computational Intelligence, 11*(1), 133-145.
22. Juma B. A., Oke A. S, Mutuku W. N., Ariwayo A. G. & Ouru O. J. (2022). Dynamics of williamson fluid over an inclined surface subject to coriolis and lorentz forces. *Engineering and Applied Science Letters, 5*(1), 37–46.
23. Nadeem, M., Siddique, I., Awrejcewicz, J., & Bilal, M. (2022). Numerical analysis of a second-grade fuzzy hybrid nanofluid flow and heat transfer over a permeable stretching/shrinking sheet. *Scientific Reports, 12*(1).
24. Siddique, I., Khan, Y., Nadeem, M., Awrejcewicz, J., & Bilal, M. (2022). Significance of heat transfer for second-grade fuzzy hybrid nanofluid flow over a stretching/shrinking riga wedge. *AIMS Mathematics.*
25. Reddy, S. C., Asogwa, K. K., Yassen, M. F., Adnan, Iqbal, Z., M-Eldin, S., Ali, B., & KM, S. (2022). Dynamics of MHD second-grade nanofluid flow with activation energy across a curved stretching surface. *Frontiers in Energy Research, 10*.
26. Koriko O. K., Adegbie K. S., Oke A. S., & Animasaun I. L. (2020). Exploration of Coriolis force on motion of air over the upper horizontal surface of a paraboloid of revolution. *Physica Scripta, 95* (035210).
27. Oke, A. S. (2022). Heat and mass transfer in 3D MHD flow of EG-based ternary hybrid nanofluid over a rotating surface. *Arabian Journal for Science and Engineering, 47*(12), 16015-16031.
28. Oke, A. S. (2017). Convergence of differential transform method for ordinary differential equations. *Journal of Advances in Mathematics and Computer Science, 24*(6), 1-17.
29. Hussain, A., Arshad, M., Rehman, A., Hassan, A., Elagan, S. K., & Alshehri, N. A. (2021). Heat transmission of engine-oil-based rotating nanofluids flow with influence of partial slip condition: A Computational model. *Energies, 14*(13), 3859.
30. Vinayagam, G., & Golla, V. K. A. (2022). Flow Transport Phenomena of a Hybrid Nanofluid Suspended by Magnetic Iron Oxide and Molybdenum Disulfide Nanoparticles in Blood Plasma. *Biointerface Research in Applied Chemistry, 13*(5), 415.
31. Khan, U., Shafiq, A., Zaib, A., Sherif, E.-S. M., & Baleanu, D. (2020). MHD Radiative Blood Flow Embracing Gold Particles via a Slippery Sheet through an Erratic Heat Sink/Source. *Mathematics, 8(9), 1597.*